Investigation of the structural determinants of the intrinsic fluorescence emission of the *trp* repressor using single tryptophan mutants

Catherine A. Royer
School of Pharmacy, University of Wisconsin-Madison, Madison, Wisconsin 53706 USA

ABSTRACT The fluorescence decay properties of wild-type *trp* repressor (TR) have been characterized by carrying out a multi-emission wavelength study of the frequency response profiles. The decay is best analyzed in terms of a single exponential decay near 0.5 ns and a distribution of lifetimes centered near 3–4 ns. By comparing the recovered decay associated spectra and lifetime values with the structure of the repressor, tentative assignments of the two decay components recovered from the analysis to the two tryptophan residues, W19 and W99, of the protein have been made. These assignments consist of linking the short, red emitting component to emission from W99 and most of the longer bluer emitting lifetime distribution to emission from W19. Next, single tryptophan mutants of the repressor in which one of each of the tryptophan residues was substituted by phenylalanine were used to confirm the preliminary assignments, inasmuch as the 0.5-ns component is clearly due to emission from tryptophan 99, and much of the decay responsible for the recovered distribution emanates from tryptophan 19. The data demonstrate, however, that the decay of the wild-type protein is not completely resolvable due both to the large number of components in the wild-type emission (at least five) as well as to the fact that three of the five lifetime components are very close in value. The fluorescence decay of the wild-type decay is well described as a combination of the components found in each of the mutants. However, whereas the linear combination analysis of the 15 data sets (5 from the wild-type and each mutant) yields a good fit for the components recovered previously for the two mutants, the amplitudes of these components in the wild-type are not recovered in the expected ratios. Because of the dominance of the blue shifted emission in the wild-type protein, it is most likely that subtle structural differences in the wild-type as compared with the mutants, rather than energy transfer from tryptophan 19 to 99, are responsible for this failure of the linear combination hypothesis.

INTRODUCTION

Time-resolved and steady-state fluorescence emission parameters are widely used observables in the study of protein stability, macromolecular equilibrium binding studies, and kinetics. This stems from the sensitivity and time scale of fluorescence emission, which are convenient for the observation of these physical events. Despite the wide use of fluorescence methodologies, the detailed mechanisms for the observed fluorescence decay parameters in a native protein or the changes upon denaturation, ligand binding, or oligomerization of proteins are not well understood. The intrinsic tryptophan decays of a number of multi-tryptophan containing proteins have recently been resolved using the single tryptophan mutants of the wild-type proteins (1–3). These single tryptophan mutants constitute novel single tryptophan proteins and comparison of their emission properties with those of previously studied single tryptophan containing wild-type proteins can aid in defining the properties of protein structure and dynamics that give rise to particular decay parameters. In addition to probing the effect of protein structure and environment on tryptophan emission, the studies on the mutants of *lac* repressor (1), T4 lysozyme (2), and glutamine binding protein (3) addressed the question of whether the observed wild-type fluorescence decay in these proteins represented a simple combination of the emission of the mutant proteins or whether interactions between the tryptophans of the wild-type or differences in the dynamic and structural properties of the single tryptophan mutants with respect to the wild-type could cause the linear combination hypothesis to fail. A deeper understanding of the inherent limitations in resolution of the decays of multiple tryptophan residues in proteins provides a framework for interpreting the intrinsic fluorescence of many important proteins that may contain more than one tryptophan and for which site-directed mutagenesis is not practical.

In this study we have examined the fluorescence decay of the *trp* repressor (TR) wild-type protein that contains two tryptophan residues per monomer. TR can exist as a dimer or tetramer (4) depending upon the concentration and solution conditions, although the tryptophan emission is almost completely insensitive to the tetramer-dimer equilibrium (4a). The structural characteristics of the tetramer are not yet known. However, the TR dimer architecture, as presented by Sigler and co-workers, can be summarized as a core protein, made up of four helices from each monomer (A, B, C, and F) and forming an interlocked helical dimer interface, and the DE helices that make up the helix-turn-helix DNA-binding domain of the protein (5). The tryptophan residues 19 and 99 are found in helices A and F, respectively, with W19 being located directly in the subunit interface and W99 packed up against the core. Intrinsic tryptophan fluorescence emission has been used to characterize the unfolding equilibria and kinetics of this protein (4a, 6, 7). In order to correlate tryptophan lifetime results with the dynamic and structural properties of the protein and to relate the fluorescence changes observed upon unfolding to changes in the environment of the two tryptophan resi-

0006-3495/92/09/741/10 $2.00

dues, it is important to attempt to assign the decay components recovered from the wild-type emission to the two tryptophan residues in the structure. The multi-emission wavelength studies of the wild-type were carried out first as a test of our ability to distinguish the relationship between recovered decay components and tryptophan residues. The emission wavelength dependence of the fluorescence decay of the single tryptophan mutants, W99F, containing only W19, and W19F, containing only W99, was examined. Since the three-dimensional structure of TR is available, one can draw certain conclusions concerning the structural features of the protein that give rise to the fluorescence emission properties of the two tryptophan residues. In addition, the hypothesis that the wild-type emission is the result of a linear combination of the fluorescence of the single tryptophan mutants can be tested.

MATERIALS AND METHODS

Site-directed mutagenesis

The mutant proteins were a gift from Dr. Craig Mann and Dr. C. Robert Matthews at the Pennsylvania State University. Full details of the mutagenesis techniques will be published elsewhere (Mann and Matthews, manuscript in preparation). Briefly, the wild-type TR gene was removed from pJPR2 (8) and inserted into the replicative form of M13mp19 DNA to produce mp19-trpR. Uracil-containing single-strand DNA was produced (9) and hybridized with the appropriate mutagenic oligonucleotide. Double-stranded DNA was used to transform competent DHF F cells (10), and the resulting viral plaques were used to prepare single-stranded DNA for sequencing and identification of the mutants (11). The mutated trprR DNA was removed from the mp19-trpR construct and recloned back into pJPR2 for protein expression.

Protein purification

The purification procedures used for the TR mutant repressor were similar to those described for the purification of wild-type TR (12). The purity of the proteins was verified by the presence of a single band on a coomasie brilliant blue stained SDS-PAGE (13). The protein concentrations were determined by UV absorbance at 280 nm (14). The calculated extinction coefficients are 27,455 M^{-1} cm^{-1} for wild-type, 16,402 M^{-1} cm^{-1} for W19F, and 16,442 M^{-1} cm^{-1} for W99F (Mann and Matthews, manuscript in preparation).

Fluorescence measurements

Steady-state fluorescence emission spectra were performed on an ISS Koala automated spectral acquisition unit (ISS Inc., Champaign, IL) with excitation from a Xenon arc lamp and the excitation monochromator set at 295 nm. The excitation and emission bandwidths were 8 nm. Time-resolved measurements were performed in the frequency domain using ISS frequency domain acquisition electronics. The excitation light was at 295 nm from the frequency doubled output of a Coherent Cavity dumped 701 dye laser excited with the 532 line of a Coherent frequency doubled mode-locked ND-YAG Antares laser (Coherent Corp., Palo Alto, CA). The reference lifetime compound was para-terphenyl with a lifetime of 1.0 ns in cyclohexane (15). Phase and modulation data were collected until errors were less than 0.3 and 0.005 degrees of phase and modulation units, respectively. Excitation was polarized at the magic angle. Solutions were less than 0.1 OD units at 295 nm. All buffers were 10 mM potassium phosphate, 0.1 mM EDTA, pH 7.6.

Data analysis

Data were analyzed with the global analysis software developed by Beechem and co-workers (16), Globals Unlimited (LFD, Urbana, IL). Generally, linking schemes involved sums of exponential decays in which lifetime values were linked across wavelengths or mutant protein data sets while pre-exponential factors were allowed to vary. Quantum yields were determined by comparing the total spectral intensity of each mutant over the range of 310 to 450 nm with that of tryptophan in water at pH 6.0, normalizing all values for differences in the total tryptophan concentration. The radiative rate constant (k_r) of the two mutants was calculated from the value of the average lifetime and the experimentally determined quantum yield (Q) (relative to tryptophan in water at pH 6.0, 0.12), as follows:

$$Q = k_r \sum_{i=1}^{n} \alpha_i \tau_i = k_r \langle \tau \rangle, \quad (1)$$

and the nonradiative decay rate contants (k_{nr}) were then extracted from the expression for the quantum yield given below:

$$Q_i = \frac{k_{r(i)}}{k_{r(i)} + k_{nr(i)}}. \quad (2)$$

These calculations were based on the assumption that for each tryptophan the radiative rate of each component was the same.

RESULTS

Fluorescence emission of wild-type TR

The frequency response of the fluorescence emission of wild-type TR shows only a small wavelength dependence (Fig. 1 *a*). Satisfactory fits of the data necessitate either a distribution of lifetimes and a single exponential decay of near 0.5 ns or sum of three exponential decays (~4–6 ns, 3 ns, and 0.5 ns). A decay model with only two exponential components yielded a global chisquare of 14. When the repressor decay is analyzed as a distribution and a single exponential, we recover a distribution near 3.1–3.2 ns at all wavelengths, but whose width increases substantially as the emission is monitored further to the red. The short component is recovered at 0.48 ns and is responsible for ~10% of the fluorescence intensity. The peak of the short component is found at 340 nm (fractions in Table 1 and DAS in Fig. 1), whereas that of the distribution is slightly blue shifted at 320 nm. The results of this fit of the data can be found in Table 1. If the decay is analyzed as a triple exponential, the chi-square increases significantly if the lifetime values are linked across wavelength. In a completely unlinked triple exponential fit of the multi-wavelength data, most of the fluorescence (60–70%) is alotted to a component between 2.6 and 3.2 ns, whose fractional contribution decreases with increasing wavelength. Between 8–27% of the fluorescence is due to a long component whose value and intensity increase with increasing wavelength. Finally, a short component of 0.33–0.67 ns is responsible for 9–15% of the light.

Tasayco and Carey (17) have shown that a dimeric chymotryptic fragment of TR containing only helices A–C (and thus only W19) exhibits ~80% of the wild-

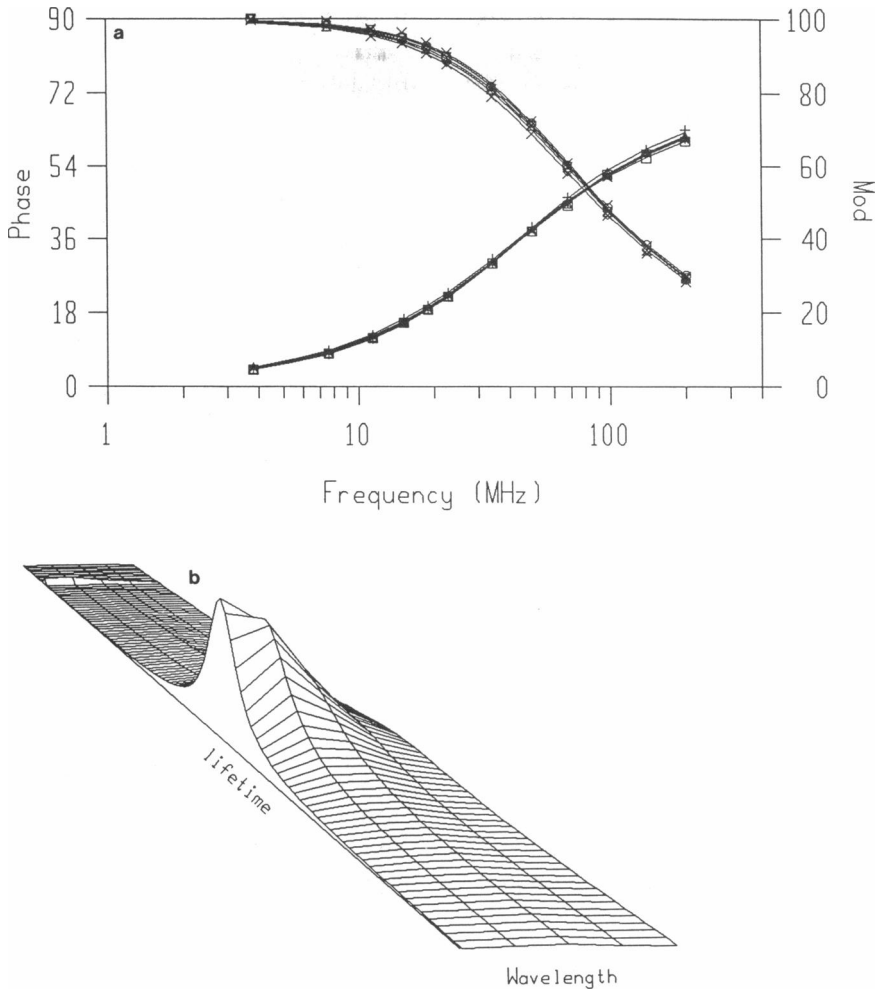

FIGURE 1 Time-resolved fluorescence of wild-type TR. (*a*) Frequency response profiles as a function of emission wavelength (320, 340, 360, 380, and 400 nm). (*b*) Decay associated spectra (DAS) recovered from the steady-state intensity values at each wavelength and the results of the distributed lifetime and single exponential analysis of the data in *a*. Frequency response profiles shift first to slightly higher and then to slightly lower frequencies with increasing wavelength.

type emission intensity. In addition, the location of this tryptophan at the subunit interface would suggest that its emission might be quite blue. W99, on the other hand, appears in the structure to be both more accessible to solvent, consistent with a redder emission spectrum. Before the single tryptophan mutants were available for studies, it appeared that the longer components arose primarily from W19 and that the 0.4–0.5-ns component was due to emission from W99. The increasing width of the distribution on the red edge and the increasing value of the longer component lifetime and fraction in the triple exponential decay, were assumed to arise from heterogeneity in W99 and W19.

TABLE 1 Results of the global analysis of the multi-emission wavelength frequency response profiles for wild-type TR as a distribution and single exponential

Wavelength (nm)	320	340	360	380	400
Chisquare	3.0	1.2	2.0	2.8	1.9
Tau1 center (ns)	3.12	3.18	3.13	3.19	3.26
Fraction	0.90	0.89	0.90	0.90	0.91
Width	0.36	0.52	0.80	0.92	1.14
Tau2 fraction (0.48 ns)	0.10	0.12	0.10	0.10	0.09

This analysis was carried out in terms of the fractional contributions of each species to the total fluorescence (f_i) at each wavelength. The global chisquare for this fit was 2.0.

Fluorescence decay parameters for TR W99F and W19F

The normalized emission spectra for TR wild-type and the two single tryptophan mutants, W99F and W19F, are plotted in Fig. 2. The wild-type spectrum resembles fairly closely that of W99F, whereas the W19F mutant exhibits a spectrum that is greatly shifted to the red with respect to the two previous spectra. The wild-type spectrum, however, clearly contains a small amount of a red emitting component emanating from W99.

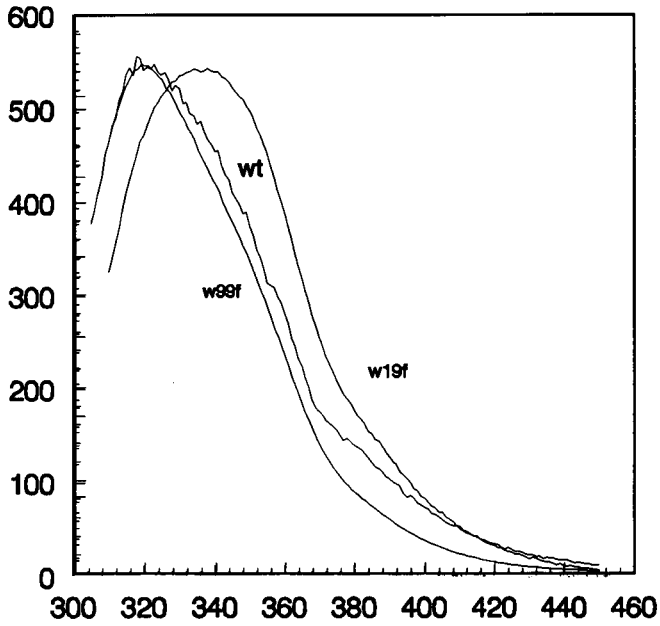

FIGURE 2 Normalized emission spectra of the wild-type TR and the two single tryptophan mutants, W19F and W99F. Excitation was at 295 nm with a xenon arc lamp and monochromator slit widths of 8 nm.

The multi-wavelength frequency response profiles of the two mutants are shown in Fig. 3, *a* and *c*. An interesting observation is that the wavelength dependence of the two mutants, particularly W19F, is much greater than that of the wild-type. This is quite the opposite of the result obtained with the *lac* repressor, in which the multi-wavelength frequency response curves for the wild-type were spread between the extremes of the two single tryptophan mutants. Analysis of the W99F mutant as a single exponential decay did not yield a satisfactory fit (global chisquare = 8.7). A double exponential decay scheme resulted in a decrease in the chisquare to 1.98, with recovered lifetime values of 4.9 and 3.2 ns. The decay associated spectra (DAS) for W99F are shown in Fig. 3 *b*. Both components exhibit a peak DAS value at 320 nm, which is the peak value of both the W99F and the wild-type spectra. The decay associated spectra for W19F are shown in Fig. 3 *d*. All three components have a peak DAS value near 340 nm, which is quite red shifted with respect to the wild-type TR spectrum in Fig. 2. The analysis of the W19F mutant required a triple exponential model for a satisfactory fit. A small amount of the emitted light was found to be due to a very long component (15.6 ns) in addition to a 3.0 and 0.5-ns component. The results of the global analysis of the individual single tryptophan mutants are summarized in Table 2.

The quantum yield properties of the tryptophans 19 and 99 as obtained from the two mutant proteins are given in Table 3. Tryptophan 19 has a very blue emission (319 nm) as compared with that of W99 (333 nm). Its quantum yield is also much larger, 2.5-fold, giving rise to its dominance of the wild-type emission, although its radiative decay rate is ~30% slower. These values were obtained assuming an average lifetime calculated from the pre-exponential concentration factors of 4.1 ns for W19 and 1.1 ns for W99. The nonradiative decay rate of W99 is approximately fourfold greater than that of W19, indicating efficient quenching by the surrounding protein matrix. The natural lifetime of the blue emitting W19 is 24 ns, whereas that of the redder W99 is 16 ns. This observation, that the buried tryptophan has a longer natural lifetime than does the more exposed tryptophan, is in contrast to the results obtained with PLA_2 (18), in which the form of the protein in which the tryptophan is exposed to water yielded a 58-ns natural lifetime, whereas the micellar immersed form yielded a natural lifetime of 34 ns. The buried tryptophan residues in RNase T1 and apo-azurin have natural lifetimes of 13 and 16 ns (19, 20), whereas the relatively red emitting tryptophan residues in T4 lysozyme single tryptophan mutants all exhibit similar spectra and natural lifetimes near 33 ns (2). There does not, thus, appear to be a general rule governing exposure of tryptophan to solvent and radiative decay rates. Apparently, the specific properties of the structural environment in which each tryptophan is found can lead to very different natural lifetimes. Examination of the structures surrounding W19 and W99 in Fig. 4, *a* and *b* reveals that the structural features of the area surrounding W19 include a large number of hydrophobic residues (leucine, valine, phenylalanine) and the indole ring here appears to be sandwiched between the F22 and H16. Since histidine is a reasonably efficient quencher, H16 could be responsible for the appearance of a shorter (2.8–3.0 ns) component in both the W99F mutant and the wild-type. W99, on the other hand, is surrounded by a surprisingly large number of charged residues. The indole ring appears to be sandwiched in between glutamate 102 and 95 with a glutamine residue to the side of the ring. There is also an asparagine residue from the other subunit in Van der Waals contact with W99. Since carboxylic acid residues are not thought to be good fluorescence quenchers due to their low electronegativity, we propose that efficient quenching is due to N32 of the other subunit. Motion of the tryptophan away from and toward this residue would give rise to the heterogeneity of the decay. Conformations in which the tryptophan is in contact with or sufficiently close to N32 would account for the 0.5-ns lifetime. The pre-exponential factor associated with the very long lifetime was only 0.1–1%. The remaining 15–29% emission components exhibit a 2.8-ns lifetime. Jardetsky and co-workers (21) have demonstrated by NMR (hydrogen exchange and lack of NOEs) that the DE helix region is relatively disordered in the native protein. Their hydrogen exchange experiments also demonstrated relatively rapidly exchanging protons in the F-helix as well. Since the F-helix is connected to the DE region, it is possible that the emission properties of W99

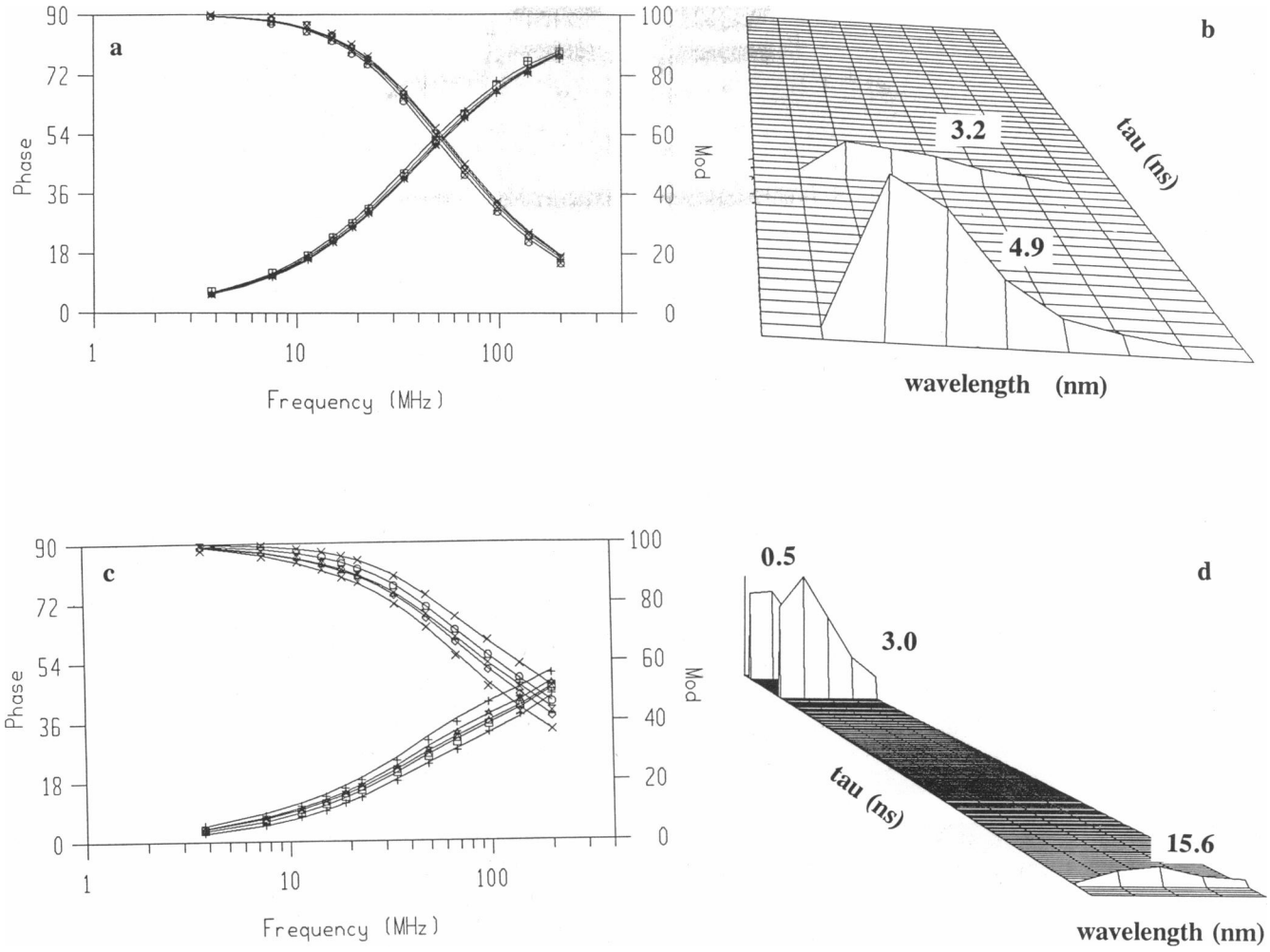

FIGURE 3 Time-resolved fluorescence of the single tryptophan mutants of TR. (*a*) W99F frequency response profiles as a function of wavelength (320, 340, 360, 380, and 400 nm). Curves shift to higher frequency with increasing wavelength. (*b*) DAS for W99F recovered from the global analysis of the double exponential decay model and the steady-state fluorescence intensity values. (*c*) W19F frequency response profiles as a function of emission wavelength (320, 340, 360, 380, and 400 nm). Frequency response shifts to lower frequencies with increasing wavelength. (*d*) DAS for W19F calculated from the fractional intensities recovered from the triple exponential decay analysis of the data and the total fluorescence intensity at each wavelength.

are a result of larger motions of the DE helices. Urea-induced unfolding of the W19F mutant (data not presented here) results in a loss of the 0.5-ns component. Presumably, this is due to a loss of contacts between the two monomeric subunits and thus abrogation of the interactions between W99 and N32 of the opposite subunit. It should be pointed out that the repressor is in equilibrium between dimers and higher order oligomers in the range of 1 to 100 μM (22). However, dilution studies of the intrinsic tryptophan lifetime and emission en-

TABLE 2 Results of the global analysis of the multi-emission wavelength frequency response profiles for TR W99F and TR W19F

Species	ns	f(320)	f(340)	f(360)	f(380)	f(400)
Tau1 W99F	4.86	0.788	0.781	0.668	0.597	0.544
Tau2 W99F	3.2	0.212	0.219	0.332	0.403	0.456
Tau1 W19F	15.56	0.006	0.036	0.07	0.076	0.107
Tau2 W19F	2.99	0.492	0.540	0.533	0.566	0.612
Tau3 W19F	0.54	0.502	0.424	0.397	0.358	0.281

This analysis was carried out in terms of the fractional contributions to the total fluorescence intensity (f_i) at each wavelength. The global chi-square value was 1.98 for the W99F mutant and 1.92 for the W19F mutant.

TABLE 3 Quantum yield and average lifetime summary for the single tryptophan mutants of TR

Mutant	W19F	W99F
Tryptophan residue No.	99	19
Position	F-helix	A-helix
Lambda max emission (nm)	333	319
Quantum yield	0.069	0.168
$\langle$Tau$\rangle$ (ns)	1.1	4.1
k_r (ns^{-1})	0.063	0.041
k_{nr} (ns^{-1})	0.85	0.20
Tau$_o$ (ns) (natural lifetime)	16	24

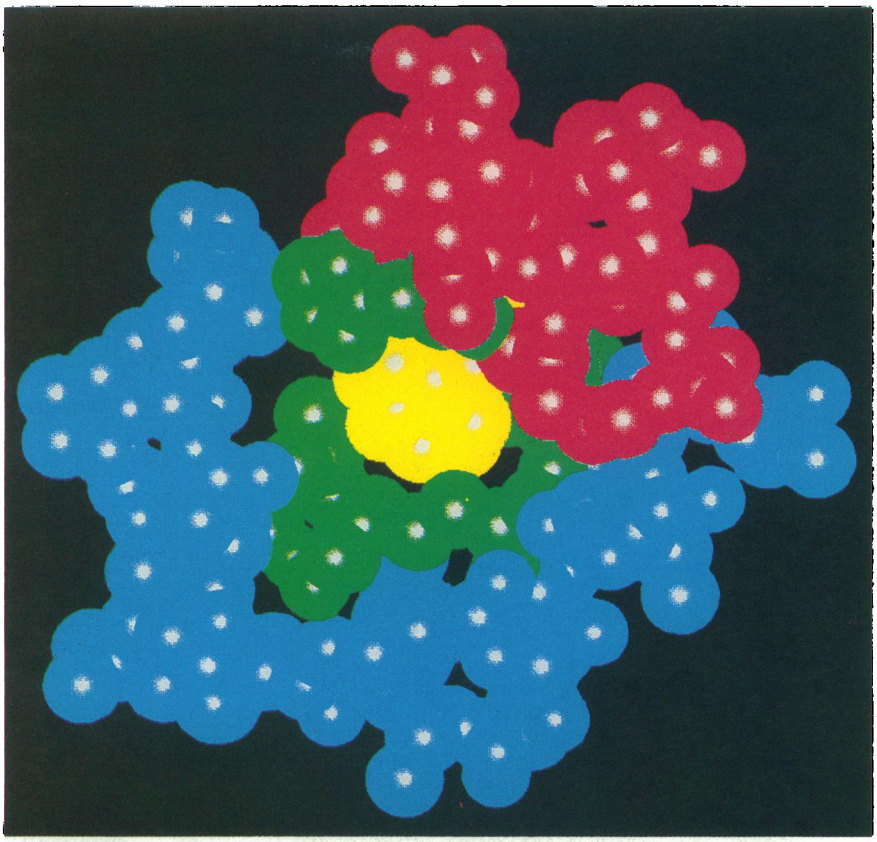

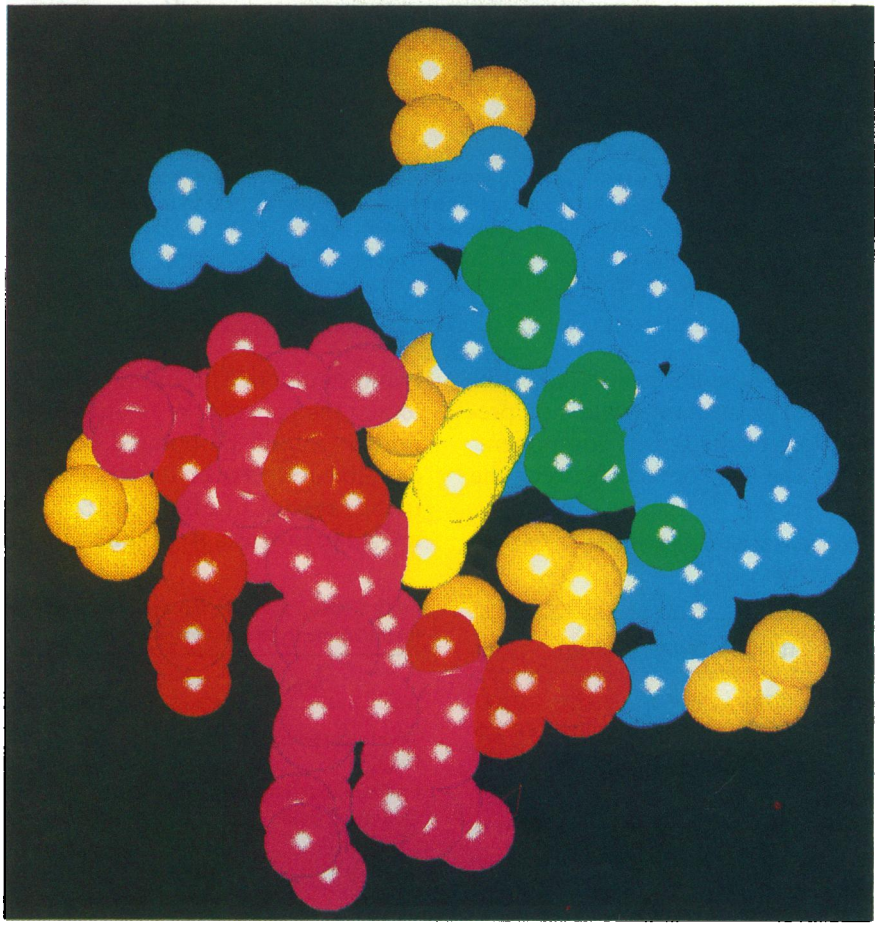

ergy (data not shown) demonstrated that the tryptophan fluorescence, with the exception of the fluorescence polarization (22) is completely insensitive to these interactions.

Thus, whereas the wild-type decays appeared to be approximately 4–6, 3, and 0.4 ns, the two mutants exhibited recovered components of near 4.9, 3.2, 15, 3.0, and 0.5 ns. It was fairly clear that the 0.5-ns component, which was well separated in value from the others in the wild-type and in W19F, was due to emission from tryptophan 99. The other components recovered from the wild-type decay might represent a mixture of the mutant decays. It was also possible that in the wild-type either structural differences with the mutants or energy transfer between W19 and W99 could result in different decays in the wild-type protein. We, therefore, carried out a global analysis in which the data for all wavelengths for the wild-type and the two mutants were analyzed in terms of a model in which the lifetime components recovered from the wild-type were constrained to be a linear combination of those present in the two single tryptophan mutants. These are the fits of the data seen in Fig. 5 *a*. The model was actually quite satisfactory and yielded lifetime components of 14.5, 4.7, 2.8, 2.6, and 0.53 ns, the first, fourth, and fifth due to W99 and the second and third due to W19. The 2.8 and 2.6-ns components were so close that their fractional contribution at 320 nm was not uniquely recovered and the values given in the DAS plots in Fig. 5 *b* represent an equalized partition of the value between the two components at that wavelength. The longest (14.5 ns) component is not included in these DAS plots so that the other components can be more easily visualized. It appears that, to a reasonable first approximation, the components present in the two single tryptophan mutants can be recovered from the wild-type decay. It was obvious from the analysis of the wild-type, even before the single tryptophan mutants became available, that the 0.5-ns component was the result of emission from W99. The hypothesis that the longer component(s) was due mostly to emission from W19 was also reasonably correct, although in the wild-type this value contains a contribution from the longer decays of W99.

The confidence interval test results for the values of the five lifetime components recovered from the global fit of the wild-type and the two mutants are given in Table 4. The value of the longest lifetime is only resolved to the extent that its lower limit is near 6 ns. The 4.6-ns component shows a 67% confidence limit between 4.3 and 6.2 ns. The confidence limits of the two 2.6–2.8-ns components overlap completely. The fact that the emission in the wild-type is so blue, however, indicates that the largest contribution is from W19. Finally, the 0.53-ns component (lifetime 5) is well resolved. These confidence limits result from complete global minimizations at each value of each parameter and thus allow for compensation due to correlations between the fitting parameters. Such a test is the most rigorous approach to evaluating the reliability of recovered fitting parameters (23). Beechem (personal communication) has demonstrated that time domain and frequency domain data sets of similar data quality (determined mostly by the quality of the pulsed light source) yield equivalent confidence limits, although the absolute chisquare values are quite different due to differences in the degrees of freedom of the analyses.

Although it appeared that the components in the mutants were present in the wild-type protein, the linear combination hypothesis requires that they be present in the amounts dictated by their contribution to the fluorescence of each mutant and the relative quantum yields of each mutant to the total wild-type emission. The spectra acquired for the two mutants and tryptophan at pH 6.0 were normalized to equivalent concentrations. Then the fractional contribution of each component in each mutant was scaled for the relative contribution expected in the wild-type emission if the linear combination hypothesis were correct. Overall, the W99F mutant, tryptophan 19, is responsible for 78% of the wild-type emission on the blue edge which decreases to 57% at 400 nm. The contribution of the 4.6-ns component would therefore be expected to be 55% of the total wild-type emission at 320 nm and 50% at 400 nm. A list of the expected relative total contributions of each mutant to the total fluorescence emission of the wild-type as well as the expected fractional contributions of each of the components of each mutant to the wild-type decay calculated from their scaled contributions to each mutant spectrum is given in Table 4. Also given in Table 4 are the actual fractional contribution values recovered from the global analysis. It can be seen that significant differences are found for the fractional contributions of lifetimes 2, 3, and 4 (4.6 and 2.8–2.6 ns, respectively).

When the global analysis is performed and the SAS values (Species Associated Spectra, or simply fractional contributions to the total intensity associated with the

FIGURE 4 Structural features of the environment of tryptophans (*a*) (*top*) 19 and (*b*) (*bottom*) 99 taken from the three-dimensional structure derived from the x-ray data of the apo-repressor by Zhang et al. (5). In *a*, tryptophan 19 is colored in yellow and the surrounding section of its subunit is colored in pink. The opposite subunit is colored in blue. Highlighted in green are the hydrophobic amino acid residues in the vicinity of W19, which include phenylalanine 16 and histidine 22 as well as a number of leucine residues. In *b*, tryptophan 99 is highlighted in bright yellow, whereas the large number of nearby leucine residues are highlighted in orange/yellow. The surrounding protein matrix from the same subunit as tryptophan 99 is highlighted in pink, whereas the other subunit is highlighted in blue. Two glutamic acid residues and an apartic acid residue from the same subunit as tryptophan 99 are colored in red, whereas the two asparagine residues from the opposite subunit are colored in green.

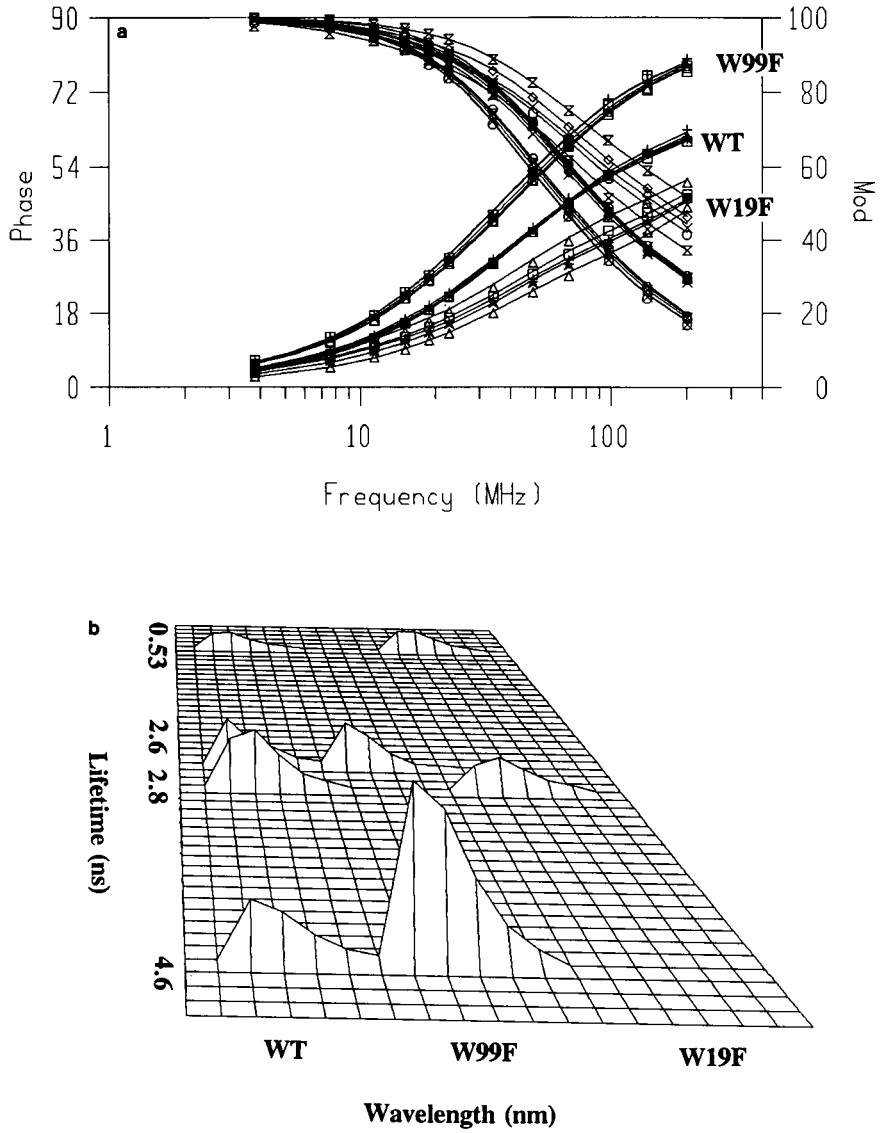

FIGURE 5 (*a*) Frequency response profiles of wild-type TR and the W19F and W99F mutants (data from Figs. 1 *a*, 3 *a*, and *c*) analyzed simultaneously constraining the wild-type emission to be a combination of emission of the two mutants. The decay scheme is further described in the text. (*b*) Decay associated spectra (DAS) of the five components in the two mutants and the wild-type, with the exception of the 14.5-ns component, which is not pictured here.

lifetime component) for the 4.6-ns component are fixed to their expected values of 0.55 to 0.5, the global chi-square for the fit increases from 1.6 to near 20. The fractional contributions of the 14.5 and 0.5-ns components have no effect on this fit. In fact, the loss of the 4.6-ns component in the wild-type is to the 2.6–2.8-ns components. This observation would explain why the analysis of the wild-type decays yielded lifetime values closer to 3 ns for the bulk of the emission, rather than the 4.6 ns found in W99F. This gain in the value of the 2.6–2.8-ns components (the loss of the 4.6 ns component is picked up by both the 2.6 and 2.8-ns components because SAS values were not uniquely resolved) to the detriment of the 4.6-ns component can be explained by energy transfer from W19 to W99 in the wild-type, which obviously does not occur in the W99F mutant. Another possibility is that the structural properties of the wild-type differ slightly from those of the mutants, such that W19 exhibits more of the shorter component, perhaps due to increased quenching by the nearby histidine residue in the structure. It is well known that mutations at positions distant to a tryptophan residue in a protein structure can cause subtle changes in the dynamics and structure of the protein which are quite easily detected by fluorescence decay measurements. The stability of the two mutants against denaturation by urea is only slightly less than that of wild-type (data not shown).

In the case of the *lac* repressor (1), no attempt was made to determine whether the components in the wild-type data were present in the ratios expected from their

TABLE 4 **Comparison between the global fit and the linear combination hypothesis for the species fractional contributions to wild-type TR fluorescence**

Species (tau)	67% confidence limit	Trp	f_i expected from quantum yield (Q)					f_i recovered from global analysis				
			320	340	360	380	400	320	340	360	380	400
ns	*ns*											
Tau2 (4.6 ns)	−0.3/+1.2	W19	0.55	0.52	0.52	0.54	0.50	0.23	0.24	0.21	0.24	0.26
Tau3 (2.8 ns)	−1.6/+1.1	W19	0.23	0.18	0.13	0.06	0.07	0.37	0.23	0.27	0.24	0.24
Tau1 (14.5 ns)	−8.0/+ >10	W99	0.00	0.01	0.03	0.03	0.05	0.0	0.0	0.02	0.03	0.04
Tau4 (2.6 ns)	−1.0/+0.8	W99	0.11	0.16	0.19	0.22	0.26	0.29	0.39	0.37	0.35	0.33
Tau5 (0.5 ns)	−0.12/+0.12	W99	0.11	0.12	0.13	0.14	0.12	0.12	0.14	0.13	0.14	0.13
Q (W19F)		W99	0.22	0.30	0.35	0.40	0.43					
Q (W99F)		W19	0.78	0.70	0.65	0.60	0.57					

quantum yield. Axelson and co-workers (3), in their studies of glutamine binding protein and its single tryptophan mutants, did attempt to do so and were unable to conclude as to the absolute validity of the linear combination hypothesis, although they found it to be quite reasonable to a first approximation. Significant errors in pipetting and determination of relative quantum yields can obscure small deviations from the linear combination hypothesis. However, in the case of TR, the deviation between the expected and recovered fractional contributions is too large to be accounted for simply by the inherent experimental error. Hudson and co-workers (2) demonstrated clearly that the linear combination hypothesis did not hold in T4 lysozyme due to energy transfer between tryptophans in the wild-type protein. In this case, it would appear that although the components in the mutants appear to be present in the wild-type, they are not present in the correct ratios. Although energy transfer cannot be completely ruled out as the basis for the failure of the linear combination hypothesis, the dominance of the blue emission in the wild-type protein argues against transfer from tryptophan 19 to 99, and in favor of the hypothesis that the loss of the 4.6-ns component is due to increased quenching of W19, resulting in an increase in the contribution of the 2.8-ns component.

CONCLUSIONS

Despite the lack of total resolution of the fluorescence decay parameters in double tryptophan proteins, it appears in general that, by careful analysis of the decay properties of the wild-type protein, a reasonable assignment of the decay components to individual tryptophan residues is possible. The resulting assignment of decay components to amino acid residues in the case of the *trp* repressor of a long (3–4 ns) blue component primarily to tryptophan 19 and a short redder emitting component (0.5 ns) to tryptophan 99 accounts for the salient features of the total wild-type fluorescence decay. The necessity of including either a distribution of lifetimes or a third intermediate species in the wild-type analysis stems from the multi-exponential character of both tryptophan decays with similar intermediate lifetime components. It follows that the observation of the evolution of these decay parameters in the wild-type protein upon changing some biophysically relevant parameter (ligand concentration, temperature, urea concentration, protein concentration), generally does provide a solid foundation for conclusions concerning which tryptophan, and therefore which part of the protein structure, is involved in the thermodynamic or dynamic phenomenon under study.

These results, however, also demonstrate clearly that not all the subtleties of the decay of the two tryptophan residues can be extracted from data on the wild-type protein. Success or failure of the linear combination hypothesis for explaining the wild-type decay is not always evident, even when the single tryptophan mutants and the three-dimensional structure of the wild-type protein are all available. In addition, as pointed out by Beechem and Brand (24), the decay of two tryptophan proteins is often apparently less complex than that of single tryptophan proteins. The work presented here and that on the previously studied two tryptophan system (1) demonstrates that this apparent simplicity is due to the collapse of multiple decay components in the wild-type into a single component or distribution. In the case of the *lac* repressor, the wild-type exhibited a well resolved 9-ns component which was also present in the W201Y mutant and clearly attributable to tryptophan 220. The 2.0-ns decay also from W220 and the 5.0 and 1.8-ns decays from W201, collapsed into an apparent 3-ns decay in the wild-type, rendering its decay less complex than that of the mutants. In the case of TR, it is the 0.5-ns component that is clearly resolved in the wild-type and in the W19F mutant. The other decays collapse into an apparent distribution of lifetimes near 3 ns. Since, however, the emission spectrum is dominated by a blue component, one can make the assumption that the bulk of the apparent distribution is from W19.

We may also make a general conclusion from the data presented here concerning the dynamic properties of W99 and its surroundings. Since the quenching of W99 is dynamic in origin, there must be motion of either the

tryptophan side chain, the nearby quenching residue, or both, which gives rise to a triple exponential decay. The short lived component (0.5 ns) of this triple exponential decay would be associated with a native or ordered structure, and the long lived (2.8 ns) component could represent a less quenched and less well ordered structure, given that the DEF unfolded fragment (17) and the unfolded wild-type protein (4a) both exhibit very little of the 0.5-ns component. This would suggest a fair degree of motion of that part of the polypeptide in the native state and is in good agreement with the NMR results of Jardetskey and co-workers (21). Further studies will include the use of the single tryptophan mutants to resolve the large changes in fluorescence that occur upon protein denaturation.

The mutant and wild-type proteins used in this study were kindly provided by Dr. Craig Mann of the laboratory of Dr. C. Robert Matthews at the Pennsylvania State University. The author would also like to thank Drs. Mann and Matthews for helpful discussions and careful reading of the manuscript.

This work was supported by the National Institutes of Health, grant GM39969 (to Catherine Royer).

Received for publication and in final form 23 March 1992.

REFERENCES

1. Royer, C. A., J. A. Gardner, J. M. Beechem, J.-C. Brochon, and K. S. Matthews. 1990. Resolution of the fluorescence decay of the two tryptophan residues if *lac* repressor using single tryptophan mutants. *Biophys. J.* 58:363–377.
2. Harris, D. L., and B. S. Husdson. 1990. Photophysics of tryptophan in bacteriophage T4 lysozymes. *Biochemistry.* 29:5276–5285.
3. Axelson, P. H., Z. Bajzer, F. G. Prendergast, P. F. Cottam, and C. Ho. 1991. Resolution of the fluorescence intensity decays of the two tryptophan residues in glutamine-binding protein from *Escherichia coli* using single tryptophan mutants. *Biophys. J.* 60:650–659.
4. Fernando, T., and C. A. Royer. 1992. The role of protein-protein interactions in the regulation of transcription by the *trp* repressor investigated by fluorescence spectroscopy. *Biochemistry.* 31:3429–3441.

4a. Fernando, T., and C. A. Royer. 1992. Unfolding of *trp* repressor studied using fluorescence spectroscopic techniques. *Biochemistry.* In press.

5. Zhang, R.-G., A. Joachimiak, C. L. Lawson, R. W. Schevitz, Z. Otwinowski, and P. B. Sigler. 1987. The crystal structure of *trp*-aporepressor at 1.8 A resolution shows how binding tryptophan enhances DNA affinity. *Nature (Lond.).* 377:591–597.
6. Lane, A. N., and O. Jardetsky. 1987. Unfolding of the *trp* repressor from *Escherichia coli* monitored by fluorescence, circular dichroism and nuclear magnetic resonance. *Eur. J. Biochem.* 164:389–396.
7. Gittelman, M. S., and C. R. Matthews. 1990. Folding and stability of *trp* aporepressor from *Escherichia coli. Biochemistry.* 29:7011–7020.
8. Paluh, J. L., and C. Yanofsky. 1986. High level production and rapid purification of the *E. coli trp* repressor. *Nucleic Acids Res.* 14:7851–7860.
9. Kunkel, T. A., J. D. Roberts, and R. A. Zakour. 1987. Rapid and efficient site-specific mutagenesis without phenotype selection. *Methods. Enzymol.* 154:367–383.
10. Hanahan, D. 1985. Techniques for transformation of *Escherichia coli. In* DNA Cloning: A Practical Approach, Vol. 1. D. M. Glover, editor. IRL Press, Oxford. 109–135.
11. Sanger, F., A. R. Coulson, B. G. Barrell, A. J. Smith, and B. A. Rose. 1980. Cloning in single-stranded bacteriophage as an aid to rapid DNA sequencing. *J. Mol. Biol.* 143:161–178.
12. Chou, W.-Y., C. Bieber, and K. S. Matthews. 1989. Tryptophan and 8-anilino-1-napthalenesulfonate compete for binding to *trp* repressor. *J. Biol. Chem.* 264:18309–18313.
13. Schagger, H., and G. von Jagow. 1987. Tricine-sodium dodecyl sulfate polyacrylamide gel electrophoresis for the separation of proteins in the range of 1 to 100 kDa. *Anal. Biochem.* 166:368–379.
14. Gill, S. C., and P. H. von Hippel. 1989. Calculation of protein extinction coefficients from amino acid sequence data. *Anal. Biochem.* 182:319–326.
15. Gratton, E., M. Limkemann, J. Lakowicz, B. P. Maliwal, H. Cherek, and G. Laczko. 1984. Resolution of mixtures of fluorophores using variable frequency phase and modulation data. *Biophys. J.* 46:479–486.
16. Beechem, J. M., E. Gratton, M. A. Ameloot, J. R. Knutson, and L. Brand. 1991. The global analysis of fluorescence decay data: second generation theory and programs. *In* Fluorescence Spectroscopy, Vol. I. Principles and Techniques. J. R. Lakowicz, editor. Plenum Publishing Corp. 241–301.
17. Tasayco, M. L., and J. Carey. 1992. Ordered self-assembly of polypeptide fragments to form native-like dimeric *trp* repressor. *Science (Wash. DC).* 255:594–597.
18. Ludescher, R. D., J. J. Wolwerk, G. H. de Haas, and B. S. Hudson. 1985. Complex photophysics of the single tryptophan of porcine pancreatic phospholipase A2, its zymogen and an enzyme/micelle complex. *Biochemistry.* 24:7240–7249.
19. James, D. R., D. R. Demmer, R. Steer, and R. E. Verral. 1985. Fluorescence lifetime quenching and anisotropy studies of ribonuclease T1. *Biochemistry.* 24:5517–5526.
20. Szabo, A. G., T. M. Stepanik, D. M. Wayner, and N. M. Young. 1983. Conformational heterogeneity of the copper binding site in Azurin. *Biophys. J.* 41:233–244.
21. Jardetsky, O., C. H. Arrowsmith, H. Zhang, and J. Czaplicki. 1992. Dynamics of protein-DNA interactions in the *trp* repressor system. *Biophys. J.* 61:1621.
22. Fernando, T., and C. A. Royer. 1992. Role of protein-protein interactions in the regulation of transcription by *trp* repressor investigated by fluorescence spectroscopy. *Biochemistry.* 31:3429.
23. Beechem, J. M. 1992. Global analysis of biochemical and biophysical data. *Methods Enzymol.* 210:37–53.
24. Beechem, J. M., and L. Brand. 1985. Time-resolved fluorescence of proteins. *Annu. Rev. Biochem.* 54:43–71.